Charge Transfer between a Gold Substrate and CdS Nanoparticles Assembled in Hybrid Organic–Inorganic Films

ARTICLE *in* THE JOURNAL OF PHYSICAL CHEMISTRY B · APRIL 2003

Impact Factor: 3.3 · DOI: 10.1021/jp022215w

6 AUTHORS, INCLUDING:

Richard W. Gurney
Simmons College
67 PUBLICATIONS **461** CITATIONS
SEE PROFILE

Meir Lahav
Weizmann Institute of Science
298 PUBLICATIONS **9,759** CITATIONS
SEE PROFILE

Sidney R Cohen
Weizmann Institute of Science
175 PUBLICATIONS **4,874** CITATIONS
SEE PROFILE

Ron Naaman
Weizmann Institute of Science
304 PUBLICATIONS **5,354** CITATIONS
SEE PROFILE

Charge Transfer between a Gold Substrate and CdS Nanoparticles Assembled in Hybrid Organic−Inorganic Films

A. Samokhvalov,[†] R. W. Gurney,[‡] M. Lahav,[‡] S. Cohen,[§] H. Cohen,[§] and R. Naaman*,[†]

Department of Chemical Physics, Department of Material and Interfaces, Chemical Services, Weizmann Institute of Science, Rehovot, 76100, Israel

Received: October 14, 2002

CdS quantum particles (QPs) assembled at predetermined distances from a gold substrate are prepared within a Langmuir−Blodgett film that forms an organic host matrix. The system is characterized by controlled surface charging (CSC) in X-ray photoelectron spectroscopy (XPS) and complementary methods, successfully resolving the discrete QP layers. A quantitative study of substrate-QPs charge-transfer channels is provided by laser-intensity dependent contact potential difference (CPD) measurements. The extracted electron-transfer rate constants exhibit marked differences in electron transfer from the film toward the substrate versus the backward process. The charging of the hybrid film was found to be either negative or positive depending on the intensity of the laser that photoexcites the QPs.

Introduction

Quantum size particles made from semiconducting material can serve in future nanosize electronics and photonics applications. In any such applications the quantum particles (QPs) will necessarily be imbedded in a matrix or solution, and hence, their properties will be altered from those of the isolated particle. Specifically, electron-transfer processes between the QPs and their surroundings can have a major effect on their optoelectronic properties.

In the present work, we investigate electron-transfer rates between a metal substrate and QPs, which are part of a hybrid inorganic/organic thin film deposited on the substrate. The inorganic components in the films are monodisperse CdS particles of quantum size, that are arranged in discrete layers. In past studies various methods were applied for investigating electrooptical properties of such hybrid films[1,2] including photoluminescence,[3−5] transient absorption,[6,7] transient excitonic bleaching,[8] valence-band photoemission,[9] and X-ray photoemission from the core levels of the QPs.[10] Charging and photoionization properties of QPs were also studied using electrostatic force microscopy.[11,12] Previously, we investigated the electronic properties of these films applying the photoemission technique.[13]

The contact potential difference (CPD) technique measures the contact potential between a known surface and that probed by varying the distance between them, hence, varying the electrical capacitance of the system. Therefore, the method is contact free. The photoattenuated CPD technique is usually applied for semiconductor surfaces. Through CPD measurements, the charge carrier lifetimes as well as the nature of the surface states can be determined in particular during a process of illumination.[14] Commonly, the illumination is performed with a continuous light source of a variable wavelength or intensity. The method is not applicable for metal surfaces, because the lifetime of the excited state is short, and hence, the excited state steady state population, obtained with a typical excitation source, is too small to affect the work function significantly. However, when the surfaces are coated with thin films, which are weakly coupled to the substrate, charge-transfer processes may occur on a long enough time scale, so that photoinduced changes in the work function can be measured.[15] The method has been applied in the past for studying films made from quantum dots of CdSe, and it was found that nonnegligible electric fields can exist in such films.[16]

In the present study, we applied lasers in combination with the CPD technique to study charge transfer between a metal substrate (gold) and a photoexcited hybrid organic/inorganic Langmuir Blodgett (LB) film containing organic amphiphiles and quantum particles (QPs) of CdS. By measuring the CPD signal as a function of the light intensity, we quantified the dynamics of the charge-transfer processes.

Experimental Section

Preparation and Characterization of the Films. Cadmium chloride (Aldrich), sodium sulfide (Aldrich), sulfuric acid (Merck), chloroform (Merck), ethanol (Merck), trifluoroacetic acid (Merck), docosanoic acid $CH_3(CH_2)_{20}COOH$ (Sigma), and 1-octadecanethiol (Aldrich) were used without additional purification. Synthesis of the thio acids was described elsewhere.[17] The gold-coated glass slides ($0.5'' \times 3'' \times 0.04''$ with 5 nm of titanium and 100 nm of gold) were purchased from EMF corporation (Ithaca, NY). The LB films for the XPS measurements were deposited on a silicon wafer coated with 5 nm of Ti and then 100 nm of Au. The (111) silicon wafer was B doped (p type) with a resistivity of 2−11 Ohm cm and thickness between 400 and 450 μm.

The monomolecular Langmuir films were prepared by spreading the solution of the carboxylic and thiocarboxylic acid mixture (90/10 and 50/50 molar ratios) in the mixed solvent (99% chloroform/1% trifluoroacetic acid) on the aqueous subphase (1 mM solution of $CdCl_2$, pH = 8.2). Immediately prior to deposition, the gold slides were cleaned with toluene in a Soxhlet extractor. Molecular layers of organic spacers of

* To whom correspondence should be addressed.
[†] Department of Chemical Physics.
[‡] Department of Material and Interfaces.
[§] Chemical Services.

10.1021/jp022215w CCC: $25.00
Published on Web 04/09/2003

SCHEME 1: Structure of the Langmuir−Blodgett Film of the Precursor

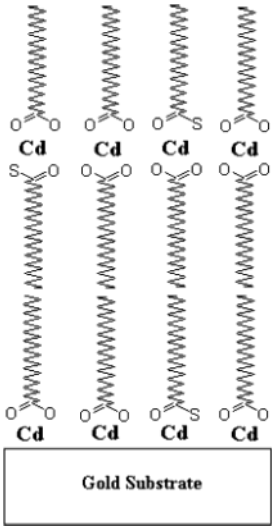

The Cd^{2+} salt in contact with substrate corresponds to the mixture of cadmium alcanoate, $Cd(C_{21}H_{43}COO)$, and cadmium thioalcanoate, $Cd(C_{21}H_{43}CSO)$. The Cd^{2+} salt further away from the surface of the substrate corresponds to the mixture of cadmium alcanoate, $Cd(C_{21}H_{43}COO)_2$, and cadmium thioalcanoate, $Cd(C_{21}H_{43}CSO)_2$.

varying thickness were prepared on the gold surface either by self-assembly (thiol C_{18}) or by the LB method (up to three bilayers of fatty acid $CH_3(CH_2)_{20}COOH$). Prior to self-assembly, the gold slides were cleaned in a UV-ozone chamber (UVOCS Inc., Montgomeryville, PA) for 20 min and then washed for 20 min with absolute ethanol.

Mixed films of cadmium docosanoate and thiodocosanoate were prepared by Langmuir−Blodgett vertical dipping deposition of the monomolecular film from the aqueous subphase (target pressure 25 mN m^{-1}, dipping rate 10 mm min^{-1}, temperature 293 K, the number of layers varied) using a KSV Langmuir minitrough. The first indication for the quality of the deposited LB films and their structure was obtained via the transfer ratio.

Formation of the QPs inside the organic matrix was achieved by a topotactic gas/solid reaction of the LB films with the H_2S (from a commercial cylinder that was dried over $CaCl_2$ and $CaSO_4$ or generated in situ by reaction of Na_2S with 20% H_2SO_4), for 4 h at room temperature. The diameter of the QPs, within the hybrid films, depends on the carboxylic/thiocarboxylic acid molar ratio, and it is either about 5 nm for the large QPs (ratio 90/10%) or about 2.5 nm for the small QPs (ratio 50/50%). For each size of the QPs, four different types of films were prepared, as shown in Scheme 2. Optionally, the spacer as in Scheme 2B may be either three bilayers of docosanoic acid or one monolayer of C18 thiol.

FT-IR spectra of the LB films were measured (1) on CaF_2 slides in transmission mode or (2) on films of gold in grazing incidence mode. UV−vis absorption spectra of the CdS QPs within the organic matrix were recorded in transmission mode on the Beckman DU-7500 spectrometer. The hybrid LB films with 5 layers of QPs were used for UV spectroscopy measurements. TEM images were taken on a Philips CM12 transmission electron microscope operated at 100 kV under low dose condition, applying a CCD camera. LB films for these experiments were deposited on collodion/carbon coated nylon grids (inert to H_2S) attached to glass slides for the dipping procedure.

XPS measurements were performed on a Kratos Analytical AXIS-HS instrument, using a monochromatized Al Kα source

SCHEME 2: Four Types of Hybrid Films that Were Investigated

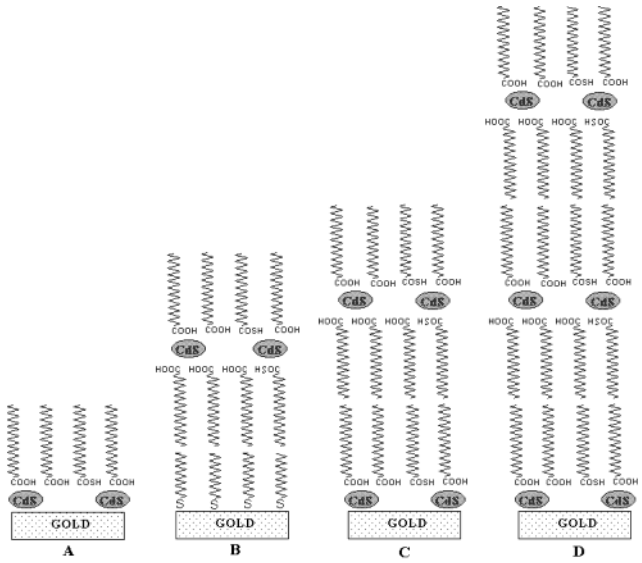

The QPs could be deposited either directly on the substrate as a single layer (A), a spacer could be placed between the first layer and the substrate (B), or the QPs could be arranged in two layers, when the first layer is on the substrate (C) or in three layers (D). The QPs in the films A−D can be either large or small. In the precursor films of the relevant structures (before QPs formation), Cd^{2+} ions are present instead of the QPs and the acid anions instead of neutral molecules.

at a relatively low power, 75 W, and pass energies ranging between 20 and 80 eV. The layered structures were studied by both angle resolved measurements and controlled surface charging (CSC).[18] Two flood-gun conditions are presented here: off and on, the latter with a negative bias voltage of 4.2 V. Accurate determination of line shifts was achieved by graphically shifting lines until a statistically optimal match was obtained. This procedure, correlating the full line shape, allowed improved accuracy in the determination of energy shifts, much beyond the experimental energy resolution (that is, source and bare line widths). Care was taken for spectral evolution with time due to beam induced damage. Each experiment included a long exposure on a fixed spot, where the spectral changes were continually followed, and then a distant fresh spot was monitored to perform measurements at optimal experimental conditions.

SFM measurements were performed on the NT-MDT P47 Scanning Force Microscope, using silicon cantilevers (NSG11 NT-MDT) with resonance frequency of 120 kHz.

CPD and Photoattenuated CPD Measurements. CPD measurements were carried out using a commercial Kelvin probe equipped with the 07 Control Electronic Unit (Besocke DeltaPhi GmbH). The measurements were performed in an ultrahigh vacuum chamber under a pressure of less than 10^{-8} Torr or under one atmosphere of nitrogen. The measurement results were performed after the signal had stabilized.

In the photoattenuated CPD measurements, the sample was illuminated by a laser beam of one of two wavelengths: ∼420 nm at 82 MHz (second harmonic of the Tsunami 100 fsec laser) or with 532 nm CW from the Millenia Nd:YAG (Spectra Physics).

The repetition rate of 82 MHz of the Tsunami laser can be regarded as quasi-CW illumination, because it is much faster than the frequency of electrical capacitance modulation in Kelvin probe (<200 Hz).

To reduce the photoinduced damage to the hybrid films, the femtosecond pulses at 420 nm (initial pulse width of about 100 fs) were temporarily stretched by passing them through 2 cm of glass.

Results

Structure of the Films. In preparing the LB films of the precursor, we aimed at obtaining the structure as shown in Scheme 1. In the preparation, two kinds of Cd^{2+} ions are anticipated. The first is formed when covering the "bare" gold substrate during the very first deposition cycle. It corresponds to the layer closest to the substrate in Scheme 1 and can be referred to as "interfacial Cd^{2+}". The chemical composition of the bottom layer was confirmed by the XPS and corresponds to the mixture of cadmium alcanoate, $Cd(C_{21}H_{43}COO)$, and cadmium thioalcanoate, $Cd(C_{21}H_{43}CSO)$. The role of the latter is to control the size of QPs by adjusting their concentration and to induce the organization of the QPs within the film.[17] The salt of the "interfacial Cd^{2+}" is formed because of the hydrophilic interaction of the Cd^{2+} ion with the metal substrate and the first layer of the docosanoic anion. It is important to note that these Cd^{2+} ions are just a few angstroms away from the metal substrate.

The second kind of Cd^{2+} salt is formed when the LB film is deposited on a substrate whose outermost layer is hydrophobic (for example, a gold substrate coated with a alkylthiol spacer). It corresponds to all but the lowest layer of Cd^{2+} salt in Scheme 1 and can be referred to as "upper Cd^{2+}". The "upper Cd^{2+}" corresponds to the mixture of cadmium alcanoate, $Cd(C_{21}H_{43}COO)_2$, and cadmium thioalcanoate, $Cd(C_{21}H_{43}CSO)_2$, as was determined previously.[17] This second kind of Cd^{2+} is at least 5 nm away from the metal substrate. To study the effect of the distance between the QPs and the substrate, we prepared three model films as shown in Scheme 2. They are

(a) 1 Layer (1L) of hybrid film with QPs directly on gold (2A);

(b) 1L of hybrid film with QPs at about 5 nm away from the gold substrate (2B);

(c) 2L of hybrid film with QPs on gold (2C).

As demonstrated in Scheme 2, the QPs in the top layer of film 2C are at about the same distance from the substrate as the QPs in film 2B (∼5 nm).

The chemical composition obtained by XPS confirms, in general, the expected structure, before and after reaction with H_2S, except for the observation of some extra signal from S atoms, found to appear at the interface with the gold substrate. With this reservation, the angular-resolved XPS (ARXPS) is consistent with the structure presented in Scheme 2. A key question, however, which is difficult to unambiguously answer by ARXPS, is the distance dependent arrangement of the QPs which have similar binding energies and line widths. Therefore, we have applied a recent modification of XPS called controlled surface charging (CSC).[18] This method, based on creation of controlled potential gradients across an overlayer, can provide in certain cases depth profiles with nanometer resolution, in a single scan.

Figure 1 shows the XPS spectrum of the Cd 3d doublet in the films with 1L of QPs directly on gold as in Scheme 2A (Figure 1A) or on the organic spacer as in Scheme 2B (Figure 1B). Upon *negative* surface charging with the flood gun (FG), the Cd line shifts toward lower binding energies. Although the magnitude of this shift is ∼2 eV in sample B, it is only ∼0.5−1 eV in A. This result reflects the role of finite electrical conductivity through the spacer molecules in sample B, as compared to the "interfacial particles", which are almost in direct contact with the grounded substrate. Figure 2 presents the response of a 2L film (Scheme 2C) to identical charging conditions as those of Figure 1. The two layers of QPs are successfully resolved. Peaks corresponding to the upper and interfacial layers of QPs are marked with arrows indicating shifts of ∼3 and ∼0.8 eV, respectively. This provides a direct proof for the arrangement of the QPs in vertically discrete layers.

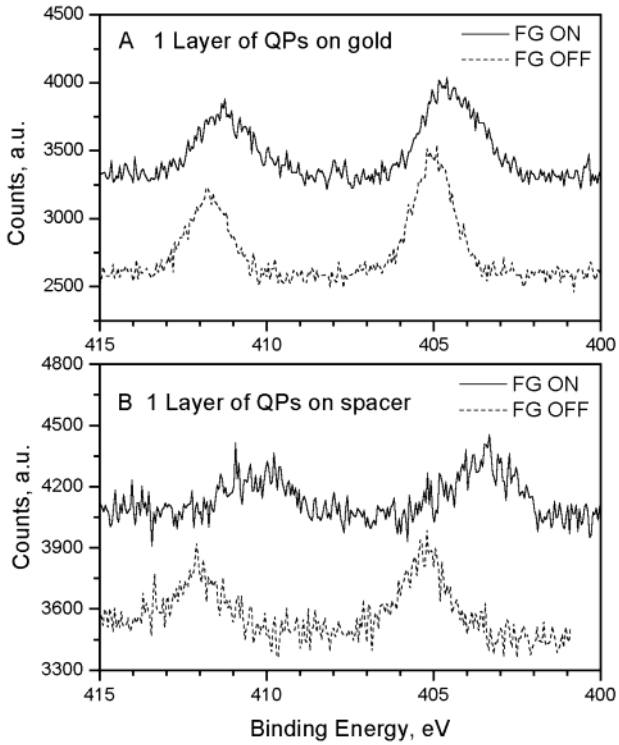

Figure 1. XPS Cd(3d) doublet, recorded from a film with a single layer of QPs: (A) in direct contact with the gold substrate, the film as in Scheme 2A; (B) located on an organic spacer, the film as in Scheme 2B. The CSC response is demonstrated, comparing spectra under flood gun (FG) off (dotted lines) and flood gun on (solid lines) conditions. Note the enhanced charging, provided by the spacer (B) as compared to the particles directly deposited on the gold (A).

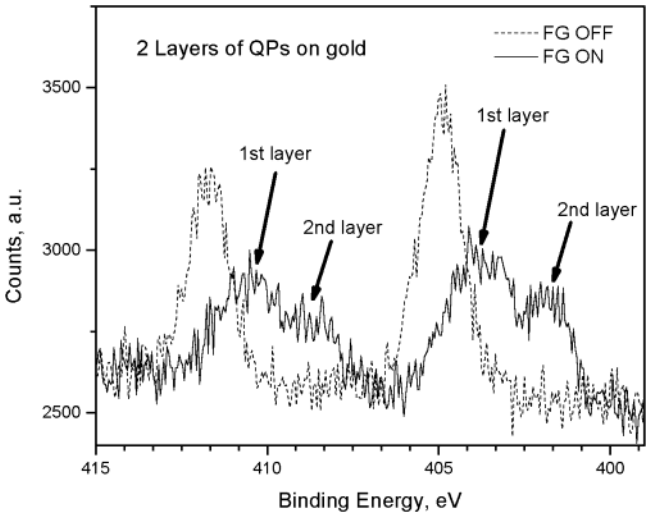

Figure 2. XPS signal of Cd(3d) doublet, taken from a hybrid film with two layers of CdS QPs, as shown in Scheme 2C. Flood gun conditions are identical to those of Figure 1. Peaks corresponding to the bottom and top layers of QPs are marked with arrows as 1 and 2, respectively.

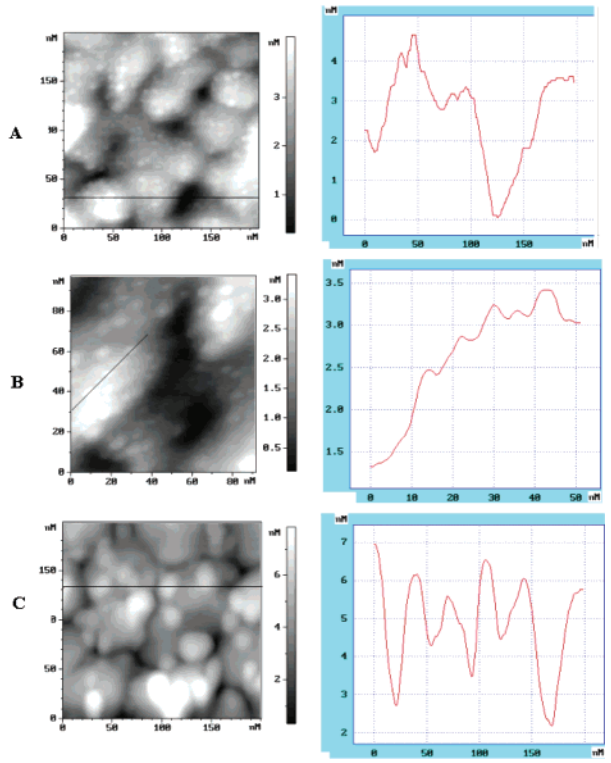

Figure 3. AFM images (on the left) and corrugation profiles (on the right) of one layer of hybrid film containing large QPs deposited directly on the gold substrate. A and B show the substrate covered with the film before rinsing with solvent, and C shows the film and substrate after rinsing. Figure 3B shows the same sample as Figure 3A but with larger magnification.

The poor quality of the present data is a result of fast scans designed to reduce beam induced damage, occurring on a time scale of minutes.[19] In Figures 1 and 2, with relatively short scans, partial damage is already recorded, expressed by the relatively low intensity of the highly charged peaks, associated with the 2nd layer (Figure 2). ARXPS data confirms that this change is not related with particle migration but to the gradual degradation in the electrical resistivity of the spacer molecules.

Positive charging of the hybrid film has been recorded as well. When the electron flood gun is switched off, the overall potential difference developed in the various overlayers is found to be 100−200 meV, evidenced by a small shift in the overlayer signals. In situ light illumination (blue-green) in the XPS is found to reduce these shifts. This result indicates that new charge-transfer channels are switched on because of photoexcitation of the QPs.[20]

The nature of the interactions of the QPs with the substrate was further characterized by AFM measurements. To probe to what extent the QPs are in contact with the gold substrate, films containing one layer of large QPs deposited on gold-coated glass slides were gently washed with an organic solvent. Before rinsing, the AFM image shows uniformly arranged QPs with average dimensions of 5 × 5 × 0.5−0.8 nm (Figure 3A). For comparison, the underlying gold film shows a much more "coarse" surface profile as also seen in Figure 3A. The typical pattern of the QPs on top of the "hill" of the substrate can be seen in Figure 3B. Swirling this film in a room temperature chloroform solution for 5 min dissolved the organic docosanoic acid/thio acid matrix. The film was dried with argon and immediately analyzed by AFM. After rinsing, the QPs remain on the surface. The size of the QPs increased due to coalescence; however, the QPs were not washed away with the organic matrix (Figure 3C).

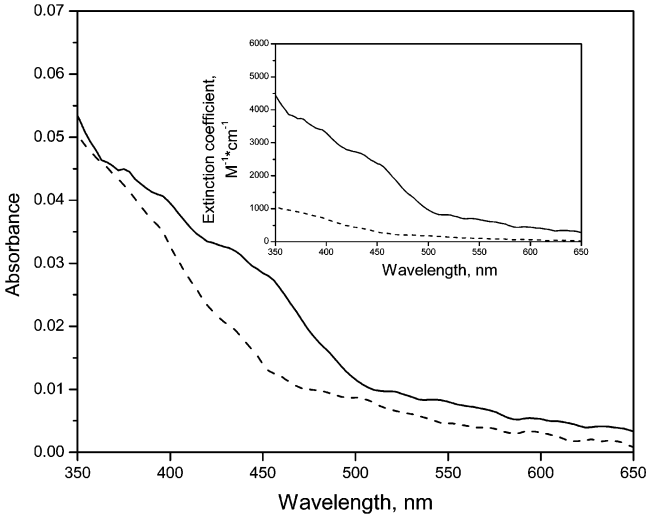

Figure 4. Absorption spectra of hybrid film with five layers of the large (solid line) and small (dashed line) QPs of CdS. The inset shows the molar extinction coefficient vs wavelength.

These results suggest that QPs layer that is the closest to the substrate may be in direct contact with the gold.

Figure 4 presents the absorption spectra of hybrid film with five layers of large or small QPs. The inset shows the molar extinction coefficient as a function of the wavelength. Optical absorption of the hybrid films in the range shown is due to the QPs only. Clearly, the large QPs absorb more at longer wavelength, as expected. These spectra are consistent with the results obtained previously with similar QPs.[17,21] The factor of ∼5 higher molar extinction coefficient for the large QPs has to do also with the higher molecular weight of the latter, compared to the small QPs.

CPD and Photoattenuated CPD Measurements. In the present study, we used a Kelvin probe for monitoring the CPD.[14] In this case, the CPD is compensated by a "backing" potential, V_b, applied during the measurements so that

$$\mathrm{CPD} + V_b = 0 \qquad (1)$$

CPD refers to the difference between the work function of the sample (hybrid film on gold in our case) and the reference golden electrode. If some extra electric charge is present on the sample, then extra potential V_{charge} is present between the electrodes. Thus, in general, eq 1 has to be modified

$$\mathrm{CPD} + V_b + V_{charge} = 0 \qquad (2)$$

For the hybrid organic−inorganic films containing QPs, the V_{charge} of the film depends on the charge transferred between the hybrid film and the substrate as a result of illumination with laser.

The photoexcitation wavelengths of 532 and 420 nm were chosen in order to correlate the data obtained by the photo attenuated CPD with the results obtained in previous studies of the hybrid films by attenuated low energy photoelectron spectroscopy.[22] Both small and large QPs can be excited by 420 nm light. However only the large QPs are excited by the 532 nm laser. Because the illumination is done with 532 nm or 420 nm, which does not photoexcite the organic matrix, photoattenuated CPD reflects the change of the charge due to excitation of the QPs *only* (note that the excitation of electron−hole pairs in the gold substrate is characterized by extremely short lifetimes). When the light is turned-off, the CPD signal is expected to return to its "dark" value. Indeed, this does happen

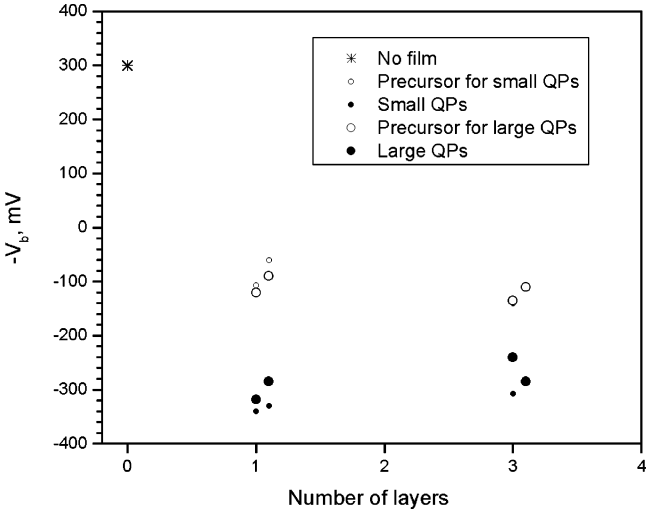

Figure 5. CPD of the hybrid films with or without QPs as a function of the number of the layers in the film. Data are presented for the substrate by itself (*), for films of the precursor of the small (○) and large (◯) QPs (before H_2S reaction), and films with the small (•) and large (●) QPs (after reaction with H_2S).

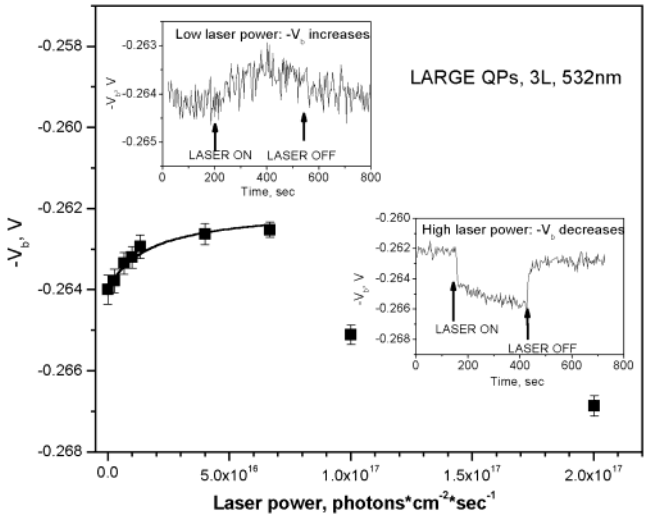

Figure 6. Photoattenuated CPD as a function of the laser power for a film with 3L of large QPs (Scheme 2D) when illuminated with a CW laser (532 nm). The experimental data are shown as large squares ■. The fit to the experimental data in the low intensity regime (based on Equation 8) is shown as a solid line. The insets show the *reversible* increase or decrease of $-V_b$ upon illumination with low and high power of laser, respectively.

but only for the hybrid films containing at least three layers of QPs. When the film of the precursor (before reaction with H_2S) is illuminated with either 532 or 420 nm light, the CPD always decreases *irreversibly*. The same is observed when the sample has just one layer of QPs (with the QPs in direct contact with the substrate).

The results are presented as the measured $-V_b$. Figure 5 shows the "dark" $-V_b$ of the hybrid films as a function of the number of the layers in the film. As in eq 1, the "dark" $-V_b$ is equal to the CPD. The $-V_b$ is shown before and after reaction with H_2S (before and after formation of QPs). The $-V_b$ decreases upon formation of the QPs and is independent of the number of layers in the hybrid film. The thickness-independent CPD implies relatively low charge mobility in the film as expected for a dielectric film.

Figure 6 shows the photoattenuated $-V_b$ as a function of the average laser power for a film with 3L of large QPs (Scheme 2D) when illuminated at 532 nm. The insets show the *reversible* increase or decrease of $-V_b$ upon illumination with low and high power intensity, respectively.

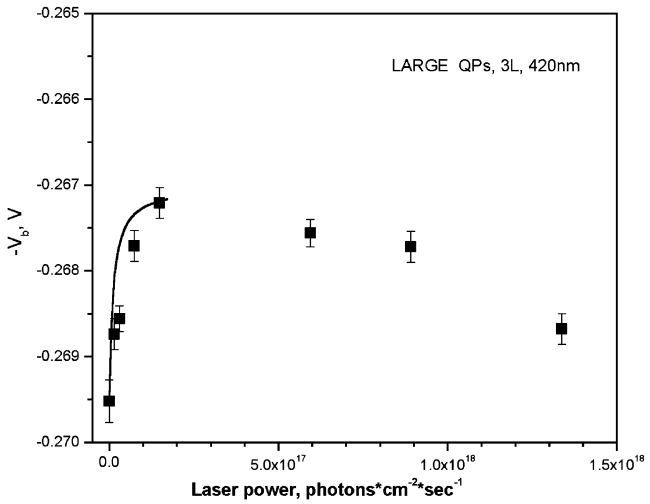

Figure 7. Photoattenuated CPD as a function of the laser power for a film containing 3L of large QPs (Scheme 2D) when illuminated with a near-UV quasi-CW laser (420 nm). The experimental data are shown as large squares ■. The fit to the experimental data in the low intensity regime (based on Equation 8) is shown as a solid line.

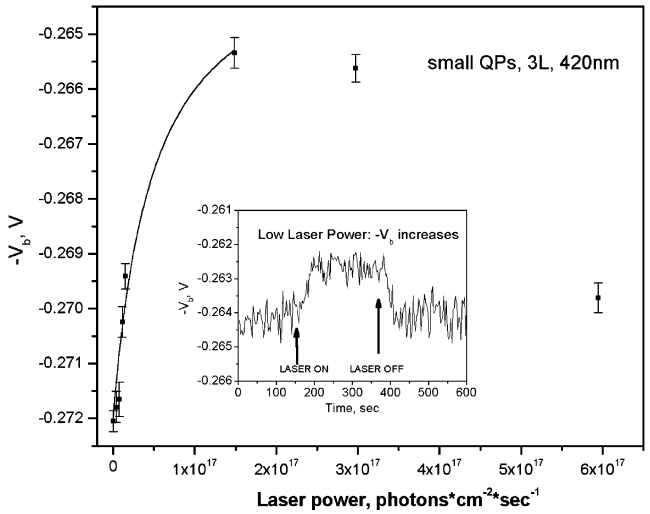

Figure 8. Photoattenuated CPD as a function of the laser power for a film containing 3L of small QPs (Scheme 2D) when illuminated with a quasi-CW laser (420 nm). The experimental data are shown as small squares ■. The fit, at the low intensity regime, to the experimental results based on eq 8 is shown as solid line. The inset shows the *reversible* increase of $-V_b$ upon illumination with low power laser.

When an organic spacer (three bilayers of docosanoic acid, >10 nm total thickness) is placed between the layers containing the QPs and the gold substrate, $-V_b$ increases upon illumination at 532 nm and the process is always *irreversible*.

Figure 7 shows the photoattenuated $-V_b$ as a function of the average laser power for a film with 3L of large QPs (Scheme 2D) when illuminated with a quasi-CW laser at 420 nm.

Figure 8 shows the $-V_b$ as a function of the average laser power for a film with 3L of small QPs (Scheme 2D) when illuminated with the same laser (420 nm). The inset shows the reversible increase of $-V_b$ upon illumination at low laser power. When illuminated with 532 nm light, the film with 3 layers of small QPs does not show any change of the $-V_b$.

By conducting the laser intensity dependent studies, we proved that multiphoton processes are of no importance in the

SCHEME 3: Energy Levels and the Electron Transfer Processes Involved in the Photoinduced Changes of the CPD of the Hybrid Films

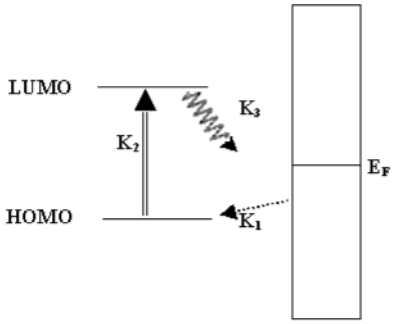

On the right, the substrate is schematically represented, whereas the HOMO and LUMO states are associated with the QPs.

current studies and start to be of significance only at much higher laser intensities.

Discussion

The present study applies macroscopic methods for investigating the charging of layers containing QPs, whereas former studies applied microscopic tools in which the single QP was probed.[11,12] Information about the electronic coupling of the QPs and the gold substrate is obtained both from the CSC−XPS and the photoattenuated CPD studies. Two cases are observed.

In the first case, there is a direct contact between the QPs and the gold substrate, as evident from the CSC−XPS and from the AFM experiments. These QPs exhibit a lesser degree of charging compared to the top QPs. Some insight on the nature of the coupling between the QPs near the substrate and the gold can be obtained from the CSC−XPS studies. The electrical conductance between the bottom QPs (Scheme 2A) and the gold is already weak, allowing the development of potential gradients of the order of 0.5 eV and more. In the second case, with a separation of ∼5 nm between the QPs and the substrate, the resistance of the organic spacer is big enough to stand much larger potential gradients, more than 2 V, though in these extreme conditions the stability of the system is quite poor.

In the photoattenuated CPD experiments, no contribution from the layer of QPs in contact with the substrate is expected, because, due to their relatively strong coupling to the substrate, the excited state lifetime is short and therefore the steady state population in the excited state, upon illumination, is very small. Indeed, the photoattenuated signal could be observed only with the three layer film. Hence, the rates obtained with the model presented below relate to charge transfer from those QPs that are not in the bottom layer.

In the case of a spacer between the QPs and the substrate (three bilayers of docosanoic acid with thickness of more than 10 nm), no charge transfer can be observed on the time scale of the experiment, as indicated by the lack of the on−off effect in the photoattenuated CPD studies. These results are consistent with former studies that also indicate that the interaction between the substrate and the QPs is very weak when separated via a long spacer.[13,22]

Scheme 3 presents the energy levels and the processes involved in the photoattenuated CPD experiments. The change in the CPD signal must result from the hybrid film being charged, either positively or negatively. The positive or negative charging of the hybrid films was independently observed in the CSC−XPS experiments (see Results).

The charging effect on the $-V_b$ signal was discussed before[23,24] for insulating films. The Kelvin probe output assumes the form

$$-V_b = \mathrm{CPD} - D\sigma e/\epsilon\epsilon_0 \tag{3}$$

where CPD is the contact potential difference between the probe and the sample before charging, σ is the surface free charge density (charge per unit area), D is the thickness of the film, ϵ is the dielectric constant of the film, e is elementary charge, and ϵ_0 is permittivity of a vacuum. From eq 3, it is clear that, if the film is charged positively, $-V_b$ will decrease, and the opposite is true for a negatively charged surface.

The laser illumination effect on the charging is described by the following simple "three state" kinetics. The rate at which the population of the ground state (N_g), HOMO in Scheme 3, is changed is given by

$$\frac{dN_g}{dt} = -K_2 I N_g + K_1(N - N_0 + N_g) = 0 \tag{4}$$

The N_0 is the initial population in the ground state, N is the population of the excited state, and I is the laser power. K_2 is the absorption cross section and was calculated from Figure 4.[25] We assume a steady-state condition during the illumination, and therefore, the charge in the excited state (LUMO in Scheme 3) is given by

$$\frac{dN}{dt} = K_2 I N_g - K_3 N = 0 \tag{5}$$

The extra charging of the film due to electron transfer from the substrate to the ground state of the photoexcited QPs is

$$N_\# = N_0 - N - N_g \tag{6}$$

When the film is charged negatively, $N_\#$ is negative. If we assume that the rate constants for charge transfer between the QP and the surface do not depend on the charging of the film (good approximation for low laser intensity), then the steady-state negative charge on the layer ($N_\#$) is given by

$$N = N_0\left[\frac{-K_2 K_3 I}{K_1 K_3 + K_2 I(K_1 - K_3)}\right] \tag{7}$$

Combining eqs 3 and 7 and noting that σ is equivalent to $N_\#$, one gets

$$-\mathrm{V_b} = \mathrm{CPD} + \mathrm{K}\left[\frac{K_2 K_3 I}{K_1 K_3 + K_2 I(K_1 - K_3)}\right] \tag{8}$$

where

$$K = D N_0 e/\epsilon\epsilon_0 \tag{9}$$

Equation 8 describes the dependence of $-V_b$ upon the laser intensity I, at the low laser intensity regime as in Figures 6−8. The observed increase of $-V_b$ at low laser powers means *negative* charging of the film.[24] Despite the very simple model, the low intensity regime in Figures 6−8 could be fitted numerically following eq 8. In the fitting procedure, we assumed $K_1 > K_3$. This corresponds to *slow* depletion of electrons from the excited state of the QPs. The rate constants obtained from the fittings are shown in the Table 1. It is important to realize that the fitting was conducted with only three variable param-

TABLE 1: Charge Transfer Rate Constants in Hybrid Films as Obtained by Numerical Fits Using Eq 8[a]

	K, Volt	K_1, 10^4 sec^{-1}	K_3, 10^2 sec^{-1}
large QP at 532 nm	0.20 ± 0.01	0.10 ± 0.01	0.10 ± 0.01
large QP at 420 nm	0.22 ± 0.01	1.00 ± 0.10	1.1 ± 0.2
small QP at 420 nm	0.89 ± 0.06	0.97 ± 0.06	0.96 ± 0.06

[a] Low laser power regime.

eters (K_1, K_3, and K), whereas one of them (K) was restricted to a narrow range of values. For each graph, at least five points were fitted.

In what follows we will discuss the ramifications of the values obtained.

(1) The constant K is related to the maximum extra charge the hybrid film can hold. It is expected to be proportional to the number of QPs. Indeed, for the hybrid films with the large particles, the value of K is by a factor 4−5 smaller than that for the films with the small QPs. This ratio is almost precisely the ratio between the number of small vs large QPs present in the films. As expected, the values of K obtained by the fitting do not vary with the photoexcitation wavelength.

(2) The rate K_1 is related to the electron transfer from the substrate to the HOMO of the QPs through the QPs/substrate interface. It is expected to be sensitive to the relative energies of the HOMO and the Fermi level of the gold substrate. As shown in Table 1, the constant K_1 is much smaller for the large QPs when excited at 532 nm, compared to the 420 nm. However, it does not vary much with the size of the QPs when excited at 420 nm. The difference in K_1 obtained for the excitation at 532 and 420 nm can be due to the fact that at 532 nm only the upper edge of the valence band (VB) is excited, whereas when excited at 420 nm, electrons from the lower energy part of VB are depleted. Hence, the filling rate for these electrons is faster. In general, the values for the electron-transfer rate constants obtained here are similar to those obtained in electrochemical studies of electron transfer between an electrode and a redox couple through self-assembled monolayers of saturated hydrocarbons.[26,27,28]

(3) The rate constant K_3 is associated with the depletion of the excited state. It is important to realize that because the experiment is not sensitive to the energy of the excited electron, but only to its presence, therefore, if the electron is relaxing to the lower energy meta-stable states on the QPs, in the model it will appear as if it is still in the excited state. The surprisingly small values of K_3 implie that indeed the electron is trapped in some excited state/s for a long time before it is transferred further to the substrate. The value of K_3 depends on the excitation energy, and as expected, for the low energy excitation, the value is smaller.

(4) It is important to realize that the low values of K_3 indicate that the depletion of the excited state by fluorescence does not take place. The assumption that luminescence quenches upon charging of the film is consistent with the previously observed blinking of the luminescence in CdSe QPs which was explained as being due to photoinduced charging/discharging of the QPs.[29]

We dealt so far with the present systems by assuming that the rate constants for electron transfer are independent of the amount of charge present on the film. Although this assumption may be valid in the low laser intensity regime, it is certainly not valid for high intensities, where charge has to flow through the already charged films. As seen in Figures 6−8, at high laser powers, $-V_b$ *decreases* with increasing laser power. This means that as more QPs are excited the charging of the films by electrons becomes less efficient, and finally, the film is even *positively* charged (Figure 6). We speculate that, at high laser powers, K_1 is reduced with respect to K_3, so that, finally, $K_1 < K_3$. The quality of numerical fitting at the high-intensity regime is by far poorer than at the low intensity region. However, the trend of "flipping" the sign of $N_\#$ toward positive values (positive charging) is obtained for high laser intensity, assuming that the rate constants are intensity dependent and $K_1 < K_3$.

It is interesting to note that photoinduced *positive* charging of the films of the CdSe quantum particles has been reported at photon fluxes close to, or above, the high power regime used in our experiments.[11] In the same work, it was observed that electron transfer between photoexcited QPs and conducting substrate can be blocked by a 5 nm thick insulating layer of silicon oxide. A similar effect is observed in the present study, where the on−off effect in the photoattenuated CPD cannot be observed for hybrid films with about 10 nm thick spacer.

Summary

We investigated quantitatively, by applying photoattenuated CPD technique, the charge-transfer processes of ordered CdS QPs within LB films of arachidic and thioarachidic acids deposited on gold substrate.

Although the photoattenuated CPD data at low laser intensities could be modeled applying a simple scheme, in the high-energy regime, the processes depend in a complex way on the laser intensity, and the model fit, although qualitatively correct, does not provide reliable rate constants. At low laser intensities, the film is charged negatively, an observation which has not been reported yet. However, a strong illumination of the hybrid films causes a decrease in the excess negative charge, until at very high illumination intensities, similar to those applied in the former studies on similar films, we indeed observe positive charging, in agreement with previous reports.

The ability to scan continuously between the two illumination regimes allowed us to obtain the rate constants for the charge-transfer processes occurring in the metal−supported hybrid films upon photoexcitation of the QPs. The charge-transfer rate constants obtained depend on the excitation wavelength. The rate for transferring electron from the excited QPs to the substrate is by far smaller than the rate for transferring charge from the substrate to the depleted HOMO on the photoexcited QPs.

Acknowledgment. A.S. and R.N. acknowledge the partial support of the Israel Science Foundation. R.G. and M.L. acknowledge support by Israel−USA Bi-National Science Foundation (BSF).

References and Notes

(1) Fendler, J. H. *Nanoparticles and nanostructured films: preparation, characterization and application*; Wiley-VCH: Weinheim, Germany, 1998.
(2) Heitmann, D.; Kottaus, J. P. *Phys. Today* **1993**, *46*, 56.
(3) Kuno, M.; Lee, J. K.; Dabbousi, B. O.; Mikulec, F. V.; Bawendi, M. G. *J. Chem. Phys.* **1997**, *106*, 9869.
(4) Micic, O. I.; Cheong, H. M.; Fu, H.; Zunger, A.; Sprague, J. R.; Mascarenhas, A.; Nozik, A. J. *J. Phys. Chem. B* **1997**, *101*, 4904.
(5) Sirota, M.; Minkin, E.; Lifshitz, E.; Henzel, V.; Lahav, M. *J. Phys. Chem. B* **2001**, *105*, 6797.
(6) Roberti, T. W.; Cherepy, N. J.; Zhang, J. Z. *J. Chem. Phys*. **1998**, *108*, 2143.
(7) Klimov, V. I.; Schwarz, Ch. J.; McBranch, D. W.; Leatherdale, C. A.; Bawendi, M. G. *Phys. Rev. B* **1999**, *60*, 2177.
(8) See, for example: Wang, Y.; Suna, A.; McHugh, J.; Hilinski, E. F.; Lucas, P. A.; Johnson, R. D. *J. Chem. Phys*. **1990**, *92*, 6927.
(9) Colvin, V. L.; Alivisatos, A. P.; Tobin, J. G. *Phys. Rev. Lett*. **1991**, *66*, 2786.
(10) Nanda, J.; Kuruvilla, B. A.; Sarma, D. D. *Phys. Rev. B* **1999**, *59*, 7473.

(11) Krauss, T. D.; O'Brien, S.; Brus, L. E. *J. Phys. Chem. B* **2001**, *105*, 1725.
(12) Krauss, T. D.; Brus, L. E. *Phys. Rev. Lett.* **1999**, *83*, 4840.
(13) Berfeld, M.; Samokhvalov, A.; Naaman, R.; Lahav, M. *Adv. Mat*. **2001**, *13*, 584.
(14) Kronik, L.; Shapira, Y. *Surf. Sci. Rep.* **1999**, *37*, 1.
(15) Moons, E.; Goossens, A.; Savenije, T. *J. Phys. Chem. B* **1997**, *101*, 8492.
(16) Kronik, L.; Ashkenasy, N.; Leibovitch, M.; Fefer, E.; Shapira, Y.; Gorer, S.; Hodes, G. *J. Electrochem. Soc.* **1998**, *145*, 1748.
(17) Guo, S.; Konopny, L.; Popovitz-Biro, R.; Cohen, H.; Porteanu, H.; Lifshitz, E.; Lahav, M. *J. Am. Chem. Soc.* **1999**, *121*, 9589.
(18) Doron-Mor, I.; Hatzor, A.; Vaskevich, A.; Van der Boom-Moav, T.; Shanzer, A.; Rubinstein, I.; Cohen, H. *Nature* **2000**, *406*, 382.
(19) This spectral evolution has been followed in detail, showing a continuous intensity shift within the broad carbon and cadmium bands, until they stabilize on their left band-edges, at ~0.5 eV potential difference from the substrate. Defects created in the organic molecules (the spacer) by the X-ray radiation gradually degrade their resistance, thus enhanced the discharge rate of the QPs.
(20) Buller, R.; Cohen, H.; Minkin, E.; Popovitz-Biro, R.; Lifshitz, E.; Lahav, M. *Advanced Functional Materials*, in press.
(21) Murakoshi, H.; Hosokawa, H.; Saitoh, M.; Wada, Y.; Sakata, T.; Mori, H.; Satoh, M.; Yanagida, S. *J. Chem. Soc., Faraday Trans.* **1998**, *94*, 579.
(22) Samokhvalov, A.; Gurney, R. W.; Lahav, M.; Naaman, R. *J. Phys. Chem. B* **2002**, *106*, 9070.
(23) Harris, L. B.; Fiasson, J. *J. Phys. C: Solid State Phys.* **1985**, *18*, 4845.
(24) Luo, G.-N.; Yamaguchi, K.; Terai, T.; Yamawaki, M. *Rev. Sci. Instrum.* **2001**, *72*, 2350.
(25) The absorption cross-sections K_2 for the large QPs is $6.0 \pm 0.7 \times 10^{-16}$ and $1.0 \pm 0.15 \times 10^{-14}$ cm^2 at 532 and 420 nm, respectively, and for the small QPs, it is $2.0 \pm 0.1 \times 10^{-15}$ cm^2 at 420 nm.
(26) Finklea, H. O. In *Electroanalytical Chemistry*; Bard, A. J., Rubinstein, I., Eds.; Marcel Dekker: New York, 1996; Vol. 19, pp 109−335.
(27) (a) Chidsey, C. E. D *Science* **1991**, *251*, 919. (b) Chidsey, C. E. D.; Bertozzi, C. R.; Putvinski, T. M.; Mujsce, A. M. *J. Am. Chem. Soc*. **1990**, *112*, 4301.
(28) Napper, A. M.; Liu, H.; Waldeck, D. H. *J. Phys. Chem. B* **2001**, *105*, 7699.
(29) Nirmal, M.; Dabbousi, B. O.; Bawendi, M. G.; Macklin, J. J.; Trautman, J. K.; Harris, T. D.; Brus, L. E. *Nature* **1996**, *383*, 802.